

Thermal conductivity of molten alkali halides from equilibrium molecular dynamics simulations

N. Galamba and C. A. Nieto de Castro

Departamento de Química e Bioquímica e Centro de Ciências Moleculares e Materiais, Faculdade de Ciências da Universidade de Lisboa, 1749-016 Lisboa, Portugal

J. F. Ely^{a)}

Chemical Engineering Department, Colorado School of Mines, Golden, Colorado 80401-1887

(Received 16 December 2003; accepted 10 February 2004)

The thermal conductivity of molten sodium chloride and potassium chloride has been computed through equilibrium molecular dynamics Green–Kubo simulations in the microcanonical ensemble (N, V, E). In order to access the temperature dependence of the thermal conductivity coefficient of these materials, the simulations were performed at five different state points. The form of the microscopic energy flux for ionic systems whose Coulombic interactions are calculated through the Ewald method is discussed in detail and an efficient formula is used by analogy with the methods used to evaluate the stress tensor in Coulombic systems. The results show that the Born–Mayer–Huggins–Tosi–Fumi potential predicts a weak negative temperature dependence for the thermal conductivity of NaCl and KCl. The simulation results are in agreement with part of the experimental data available in the literature with simulation values generally overpredicting the thermal conductivity by 10%–20%. © 2004 American Institute of Physics. [DOI: 10.1063/1.1691735]

I. INTRODUCTION

The experimental measurement of the thermal conductivity of high-temperature molten salts is very difficult because of their high melting temperatures and chemical activity. It is not surprising, therefore, that there are substantial disparities in the reported experimental results for these materials. These disparities are normally attributed to convective and radiative effects in some experimental methods. For the particular case of molten alkali halides, part of the experimental data available in the literature show an increase of thermal conductivity with temperature,¹ a behavior considered to be an *intrinsic* characteristic of molten salts.^{1,2} The experiments of Nagasaka *et al.*³ on the thermal diffusivity of molten alkali halides, however, show a weak negative temperature dependence for the thermal conductivity. Further, their values for the thermal conductivity are significantly lower than those obtained by Smirnov *et al.*¹

Molecular dynamics (MD) simulations avoid the experimental problems referred to previously and provide an alternative to obtain the thermal conductivity of molten salts. The objective of this work is to investigate the temperature dependence of the thermal conductivity of the Born–Mayer–Huggins–Tosi–Fumi (BMHTF) potential⁴ for molten alkali halides using Green–Kubo equilibrium molecular dynamics (EMD) simulations.

The thermal conductivity of molten alkali halides has been simulated by EMD before, but the results were inconclusive as to whether the temperature dependence predicted by the BMHTF potential is positive or negative. Sindzingre and Gillan⁵ performed EMD simulations using the Green–

Kubo method in the canonical ensemble (N, V, T) of the thermal conductivity of solid NaCl and KCl, but only one state point was reported for the liquid state. Fuchiwaki and Nagasaka⁶ reported EMD (N, V, E) simulations of the thermal conductivity for different molten alkali halides. The results of those simulations underpredict the thermal conductivity and were inconclusive regarding the temperature dependence of the thermal conductivity. In particular, the values reported from those simulations show positive and negative changes for the thermal conductivity of NaCl and KCl as the temperature is increased. Takase *et al.*⁷ reported extensive EMD (N, V, E) calculations for the thermal conductivity of a number of molten alkali halides. Their results overpredict the thermal conductivity and again for almost every substance, including NaCl and KCl, an alternating positive and negative temperature dependence of the thermal conductivity is observed within 100 K temperature intervals.

Because of the abnormal behavior reported in these simulations, we investigate here the temperature dependence of the thermal conductivity for molten sodium and potassium chloride. We note that Takase *et al.*⁷ have used an Ewald-energy flux expression derived by Bernu and Vieillefosse⁸ for the particular case of the one-component plasma model. In this work we give an expression for the energy flux of a binary ionic system by analogy with the expression for the stress tensor elements derived by Nose and Klein⁹ and Heyes (NKH).¹⁰ This formula is very efficient, eliminating the double sum over particles inside the Fourier space vectors sum in analogy with the case of the potential energy and forces.¹¹

Nonequilibrium molecular dynamics (NEMD) simulations for the thermal conductivity and cross coefficients have also been reported for ionic systems,^{12–14} but not for molten

^{a)} Author to whom all correspondence should be addressed. Electronic mail: jely@mines.edu

alkali halides. We note that even though NEMD has been the preferred method in the most recent studies of thermal transport coefficients, neither it nor EMD have been explored to any great extent for the case of ionic fluids.

This paper is organized as follows: First the expressions used in the calculation of the thermal conductivity through EMD with the Green–Kubo method are given. Special attention is given to the form of the microscopic energy flux for ionic systems for which the Coulombic interactions are calculated through the Ewald method. The nonpairwise nature of the reciprocal space forces in this method forces the dyadic product between force and distance to be computed as a whole in the Fourier space in analogy with the potential term of the stress tensor of an ionic system. This expression is given here by analogy with the case of the stress tensor elements and it is suitable for the MD simulation of the thermal conductivity of ionic and dipolar fluids modeled with partial charges. The details of the simulations are then discussed and the results are compared with available experimental data and previous simulation results. Finally the conclusions of this study are given.

II. THERMAL CONDUCTIVITY RELATIONS

Since the electroneutrality condition for a Coulombic system implies a constant composition, the Gibbs phase rule says that pure molten salts are one-component systems (only one chemically independent species). From this definition of a molten salt no thermal diffusion is expected to occur for a pure molten salt in analogy with the case of a one-component neutral system. Consistency with this definition was reported by Bresme *et al.*¹³ where the thermal diffusion of a binary system was calculated through NEMD as a function of the charge strength of the species, and the range of the ionic potential using Coulombic and Yukawa long-range tails, in the limits of a two-component mixture (zero charged species) and a one-component system (unit charged species). The results of this investigation showed thermal diffusion to decrease with increasing charge strength from a positive value to a negative, close to zero value (within statistical uncertainty), for a Coulombic long-range tail. For pure molten salts, however, coupled thermo-electric effects occur. The coupling of heat and charge currents in a molten salt lead to a treatment of these systems analogous to that followed for real mixtures and in this work molten NaCl and KCl were treated as binary ionic mixtures.

Thus, the relations discussed in the following are given for a binary system for which no viscous forces, external magnetic fields, or electronic current occurs and no chemical reactions take place between its components.

A. Phenomenological relations

The linear phenomenological relations that express the transport of heat and charge in a “binary” ionic system can be given by^{5,8,15}

$$\mathbf{J}_Z = -L_{ZZ}\mathbf{X}_Z - L_{ZQ}\mathbf{X}_Q, \quad (1)$$

$$\mathbf{J}_Q = -L_{QZ}T\mathbf{X}_Z - L_{QQ}\mathbf{X}_Q,$$

where \mathbf{J}_Z and \mathbf{J}_Q are the charge flux and the heat flux, $L_{\alpha\beta}$ ($\alpha, \beta = Z, Q$) are the phenomenological coefficients, and \mathbf{X}_Z and \mathbf{X}_Q are the thermodynamic forces, which are given by

$$\mathbf{X}_Z = \nabla_T(\mu_Z), \quad (2)$$

$$\mathbf{X}_Q = \nabla T.$$

In Eq. (2) $\mu_Z = (\mu_1^Z - \mu_2^Z)/(z_1 - z_2)$ where μ_k^Z is the electrochemical potential of component k , $\mu_k^Z = \mu_k + z_k\phi$ (composed by a chemical part μ_k and the electric potential ϕ ; z_k is the charge per unit of mass of component k) and the gradient is to be taken at isothermal conditions.

From the Onsager reciprocal relations¹⁶ for the cross coefficients, $L_{ZQ} = L_{QZ}$, and therefore only three independent coefficients are involved in Eq. (1). Elimination of \mathbf{X}_Z in the equation for \mathbf{J}_Q and using $\mathbf{X}_Q = \nabla T$, permits one to rewrite the heat flux relation in the following form:⁸

$$\mathbf{J}_Q = TL_{QZ}\mathbf{J}_Z/L_{ZZ} - \lambda\nabla T, \quad (3)$$

where λ is the thermal conductivity corresponding to $\mathbf{J}_Z = 0$ and is given by

$$\lambda = L_{QQ} - L_{QZ}^2/L_{ZZ}. \quad (4)$$

Notice that for $\mathbf{J}_Z = 0$, Eq. (3) becomes the well-known Fourier law of heat conduction. Further, L_{ZZ} can be identified as being the electrical conductivity σ , defined as the ratio of the electric current density, \mathbf{J}_Z , and the negative gradient of the electrochemical potential at constant temperature.⁵ Notice that if the chemical potential is constant then Ohm’s law, $\mathbf{J}_Z = \sigma\mathbf{E}$, is obtained by separating the electrochemical potential into its chemical and electrical parts.

For simulation purposes it is preferred to define the thermal conductivity in terms of the energy flux rather than the heat flux, because the latter is more difficult to calculate as discussed in the following. The two are related by

$$\begin{aligned} \mathbf{J}_Q &= \mathbf{J}_E - \sum_{k=1}^2 h_k \mathbf{J}_k = \mathbf{J}_E - (h_1 - h_2)\mathbf{J}_1 \\ &= \mathbf{J}_E - \frac{(h_1 - h_2)}{(z_1 - z_2)} \mathbf{J}_Z = \mathbf{J}_E - h_Z \mathbf{J}_Z, \end{aligned} \quad (5)$$

where h_k is the partial specific enthalpy of component k , \mathbf{J}_1 is the flux of ions of species 1 in the center of mass frame, z_k is the charge per unit mass of component k and the fact that for a binary mixture $\mathbf{J}_1 = -\mathbf{J}_2$ and $\mathbf{J}_Z = \mathbf{J}_1(z_1 - z_2)$ were used.¹⁵ Using this we can re-derive the phenomenological laws in terms of the fluxes of charge and energy.^{5,8} The new expressions are given by

$$\mathbf{J}_Z = -L_{ZZ}\mathbf{X}_Z^0 - L_{ZE}\mathbf{X}_Q, \quad (6)$$

$$\mathbf{J}_E = -L_{EZ}T\mathbf{X}_Z^0 - L_{EE}\mathbf{X}_Q$$

in which \mathbf{X}_Q has not been changed but \mathbf{X}_Z^0 is now given by

$$\mathbf{x}_Z^0 = T \nabla \left(\frac{\mu_Z}{T} \right). \quad (7)$$

This transformation leaves all physical results unchanged although a different form for the entropy production is obtained.¹⁵ For a binary mixture this transformation, Eq. (5), excludes the enthalpy flux contribution associated with the interdiffusion of one species through the other from the energy current.¹⁵ The following thermodynamic relation was used:

$$T \nabla \left(\frac{\mu_Z}{T} \right) = \nabla_T \mu_Z - \frac{h_Z}{T} \nabla T \quad (8)$$

and the relations between the two sets of coefficients are given by

$$\begin{aligned} L_{QQ} &= L_{EE} - 2L_{EZ}h_Z + \frac{L_{ZZ}}{T}h_Z^2, \\ L_{QZ} &= L_{EZ} - h_Z \frac{L_{ZZ}}{T}. \end{aligned} \quad (9)$$

Notice that the form of the phenomenological laws is unchanged under the transformation and the following expression can be obtained for the thermal conductivity:

$$\lambda = L_{EE} - \frac{L_{EZ}^2 T}{L_{ZZ}}. \quad (10)$$

Alternatively this expression can be obtained simply by substitution of Eq. (9) into Eq. (4). For the simulation of the thermal conductivity of solid alkali halides it has been shown⁵ that this transformation causes a problem in that the autocorrelation function of the energy current shows an oscillatory behavior arising from the fluctuations of the electric current at the transverse optic frequency. This problem disappears in the liquid state and the thermal conductivity can be calculated from Eq. (10).

Finally the transport coefficients involved in Eq. (10) can be computed through EMD in conjunction with the Green–Kubo method. The Green–Kubo formulas that express these three transport coefficients as time integrals of the correlation functions of microscopic fluxes are

$$\begin{aligned} L_{ZZ} &= \frac{1}{3VkT} \int_0^\infty \langle \mathbf{j}_Z(t) \cdot \mathbf{j}_Z(0) \rangle dt, \\ L_{EZ} &= \frac{1}{3VkT^2} \int_0^\infty \langle \mathbf{j}_E(t) \cdot \mathbf{j}_Z(0) \rangle dt, \\ L_{EE} &= \frac{1}{3VkT^2} \int_0^\infty \langle \mathbf{j}_E(t) \cdot \mathbf{j}_E(0) \rangle dt, \end{aligned} \quad (11)$$

where $L_{ZZ} (= \sigma)$ is the electrical conductivity, L_{EZ} is a cross thermoelectric coefficient, and L_{EE} would correspond to the thermal conductivity of a neutral one-component fluid.

B. Microscopic fluxes

The microscopic fluxes of charge \mathbf{j}_Z and heat \mathbf{j}_Q can be given by

$$\begin{aligned} \mathbf{j}_Z &= \sum_{i=1}^N Z_i e \mathbf{v}_i(t), \\ \mathbf{j}_Q &= \frac{d}{dt} \sum_{i=1}^N \mathbf{r}_i (E_i - h) \end{aligned} \quad (12)$$

with

$$(E_i - h) = \left\{ \frac{1}{2} m_i v_i^2 + \frac{1}{2} \sum_{j \neq i}^N u_{ij}(r_{ij}) \right\} - h, \quad (13)$$

where \mathbf{v}_i is the velocity of particle i , $u(r_{ij})$ the pair potential between particles i and j , \mathbf{r}_i the position vector of particle i , and h is the enthalpy per particle.¹⁷

Taking the time derivative of Eq. (13) gives the following result for the heat flux:

$$\mathbf{j}_Q = \sum_i^N \mathbf{v}_i E_i + \frac{1}{2} \sum_i^N \sum_{j \neq i}^N \mathbf{r}_{ij} (\mathbf{F}_{ij} \cdot \mathbf{v}_i) - \sum_i^N \mathbf{v}_i h. \quad (14)$$

If the total linear momentum in a single component system is zero, the last term of this expression is also zero. For a binary mixture the expression must be extended as follows:¹⁸

$$\begin{aligned} \mathbf{j}_Q &= \sum_{\alpha=1}^2 \sum_i^{N_\alpha} (E_{i\alpha} - h_\alpha) \mathbf{v}_{i\alpha} \\ &+ \frac{1}{2} \sum_{\alpha=1}^2 \sum_{\beta=1}^2 \sum_i^{N_\alpha} \sum_{j \neq i (\alpha=\beta)}^{N_\beta} \mathbf{r}_{i\alpha, j\beta} (\mathbf{F}_{i\alpha, j\beta} \cdot \mathbf{v}_{i\alpha}), \end{aligned} \quad (15)$$

where h_α is the partial enthalpy per particle of species α . The enthalpy term cannot be dropped for a binary mixture because of the different masses of the two species. The fluxes \mathbf{j}_Z and \mathbf{j}_Q have been written for a zero (“barycentric”) center of mass velocity \mathbf{u} , given by¹⁵

$$\mathbf{u} = \left(\sum_{\alpha=1}^2 \sum_{i=1}^{N_\alpha} m_{i\alpha} \mathbf{v}_{i\alpha} \right) / \sum_{\alpha=1}^2 \sum_{i=1}^{N_\alpha} m_{i\alpha}. \quad (16)$$

Because of the difficulty of calculating the partial enthalpies in MD simulations the energy flux is used instead (this is possible under the transformation previously performed on the phenomenological laws and also possible for the microscopic currents), which is given by Eq. (15) except for the enthalpy term. Notice further that for the case of pure molten salts partial thermodynamic quantities cannot be defined in the same way they are defined for neutral binary mixtures because of the fixed composition imposed by the electroneutrality condition.

For the case of a molten alkali halide it is preferred to use the energy flux in the following form:

$$\mathbf{j}_E = \frac{1}{2} \sum_{i=1}^N \left[m_i v_i^2 + \sum_{j \neq i}^N u(r_{ij}) \right] \mathbf{v}_i + \frac{1}{2} \sum_{i=1}^N \sum_{j \neq i}^N (\mathbf{r}_{ij} \mathbf{F}_{ij}) \cdot \mathbf{v}_i. \quad (17)$$

The mixture notation has been dropped for sake of simplicity with the understanding that the sums are to be performed for two different species with different masses. In Eq. (17) the term $\mathbf{r}_{ij} \mathbf{F}_{ij}$ is a dyad given by

$$\vec{S} = \begin{pmatrix} S_{ij}^{xx} & S_{ij}^{xy} & S_{ij}^{xz} \\ S_{ij}^{yx} & S_{ij}^{yy} & S_{ij}^{yz} \\ S_{ij}^{zx} & S_{ij}^{zy} & S_{ij}^{zz} \end{pmatrix} \quad (18)$$

with

$$S_{ij}^{\alpha\beta} = \sum_{\mathbf{n}} F_{ij}^{\alpha}(\mathbf{r}_{ij} - \mathbf{n}L)(r_{ij}^{\beta} - n_{\beta}L), \quad (19)$$

where L is the length of the side of the MD box and \mathbf{n} is the periodic boundary conditions translational vector ($\mathbf{n}=0, \pm 1, \pm 2, \dots$). The sum over the lattice vectors \mathbf{n} has been explicitly included in Eq. (19) to point to the fact that for an ionic system treated with the Ewald sum, the separation of the force in a real space part and a reciprocal space part, requires the sum $[\sum_{\mathbf{n}} F_{ij}^{\alpha}(\mathbf{r}_{ij} - \mathbf{n}L)(r_{ij}^{\beta} - n_{\beta}L)]$ to be treated as a whole in the Fourier space (F_{ij}^{α} is the α component of the reciprocal space force between particle i and j and all its images considered within the chosen truncation scheme for the Fourier lattice). If the forces were calculated isolated in the Fourier space and then multiplied by the distances between particles in the MD box, these would not correspond to the interactions accounted for in the reciprocal space lattice. This problem was first encountered by Bernu and Vieillefosse,¹⁹ who have shown that even though the Green-Kubo relations for the transport properties of nonionic fluids could also be applied to case of a one-component plasma, some care had to be taken in defining the microscopic currents to avoid divergences. Their derivation was given explicitly for the case of the one-component plasma using the Ewald method given by Nijboer and De Wette.²⁰ The problem was later considered for the case of viscosity^{9,10} and an efficient expression proposed for the product of the distances with the reciprocal space part of the force for monatomic and polyatomic systems, for the particular case of the stress tensor. These same expressions are to be used in the simulation of the viscosity of any dipolar fluid for which partial charges are added (e.g., liquid methanol²¹). Recently the authors have given a detailed discussion on this calculation for the case of the stress tensor elements for an ionic system for which the Ewald sum is used to calculate the Coulombic long-range forces.²²

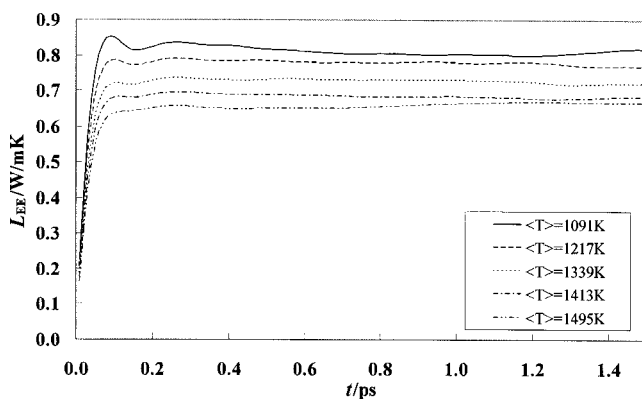


FIG. 1. L_{EE} coefficient for the different state points simulated for sodium chloride.

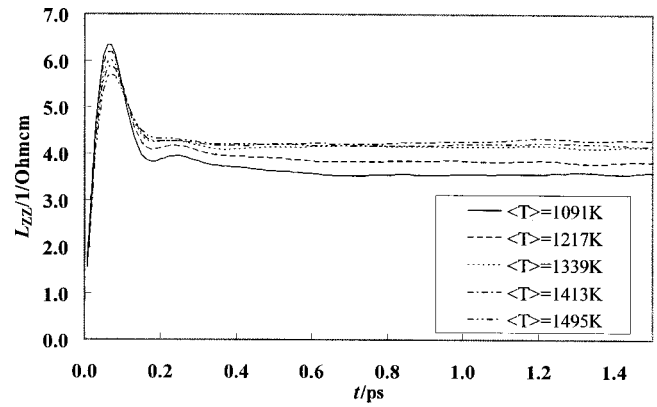


FIG. 2. L_{ZZ} coefficient for the different state points simulated for sodium chloride.

The motivation for writing the energy flux in the form given by Eq. (17) is that the sum $\sum_{j \neq i}^N \mathbf{r}_{ij} \mathbf{F}_{ij}$ is equal to the sum that arises in the definition of the stress tensor and the NKH expression to evaluate this product can be used in the thermal conductivity calculations. The final expression for the microscopic energy flux of an ionic system treated with the Ewald sum is then

$$\mathbf{j}_E = \frac{1}{2} \sum_{i=1}^N \left[m_i v_i^2 + \sum_{j \neq i}^N u(r_{ij}) \right] \mathbf{v}_i + \frac{1}{2} \sum_{i=1}^N \sum_{j \neq i}^N (\mathbf{r}_{ij} \mathbf{F}_{ij}^R) \cdot \mathbf{v}_i + \frac{1}{2} \sum_{i=1}^N \sum_{j=1}^N \mathbf{v}_i \cdot \vec{S}_{ij} \quad (20)$$

with

$$S_{ij}^{\alpha\beta} = \frac{4\pi}{L^3} \sum_{\mathbf{k} \neq 0} B_{\alpha\beta} \frac{1}{k^2} e^{-k^2/4\alpha^2} Z_i Z_j \cos(\mathbf{k} \cdot \mathbf{r}_{ij}) \quad (21)$$

and for the $\alpha\beta$ component of the tensor $\mathbf{B}(\mathbf{k})$,¹⁰

$$B_{\alpha\beta} = \delta_{\alpha\beta} - \frac{2|\mathbf{k}_{\alpha}||\mathbf{k}_{\beta}|}{|\mathbf{k}|^2} - \frac{|\mathbf{k}_{\alpha}||\mathbf{k}_{\beta}|}{2\alpha^2}, \quad (22)$$

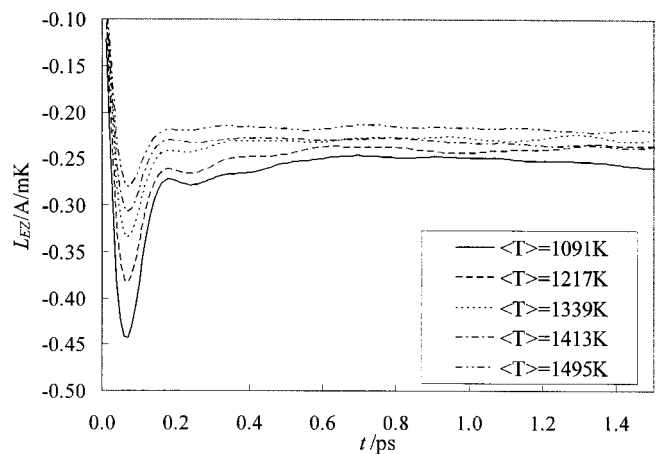


FIG. 3. L_{EZ} coefficient for the different state points simulated for sodium chloride.

TABLE I. Results for the Green–Kubo coefficients of NaCl. The correlation functions were evaluated from 5 ns production runs (5×10^6 time origins) and a time window of 5 ps.

T (K)	$\langle T \rangle$ (K)	ρ (g cm $^{-3}$)	L_{EE} (W/m K $\pm\sigma$)	$L_{ZE}^2 T/L_{ZZ}$ (W/m K)
1100	1091	1.5420	0.798 ± 0.009	0.189
1200	1217	1.4878	0.77 ± 0.01	0.19
1300	1339	1.4335	0.73 ± 0.01	0.18
1400	1413	1.3793	0.686 ± 0.005	0.181
1500	1495	1.3250	0.680 ± 0.009	0.187

where α is the convergence parameter of the Ewald sum, and $\delta_{\alpha\beta}$ is the Kronecker delta. In Eq. (20) \mathbf{F}_{ij}^R represents the short-range forces and the real part of the Ewald–Coulomb forces, both computed in the real space.

This formula is suitable for simulation of both binary “mixtures” of positive and negative ionic particles and dipolar systems modeled with partial charges. For the case of dipolar molecules or polyatomic ions an additional term should be taken into account, which handles the product of the distances and the intramolecular forces. Notice further that the Fourier part of this expression, Eq. (19), can be transformed into a much more efficient form (not given here), in the same way as the potential energy,¹¹ which eliminates the double loop over particles inside the \mathbf{k} -space triple sum.

We note that the expressions used in this work are consistent with the expressions used by Bresme *et al.*¹³ for the product $F_{ij}r_{ij}$ in the real and reciprocal space but not with the formula used by Motoyama *et al.*¹⁴ for the computation of the thermal conductivity of UO_2 .

III. SIMULATIONS

The simulations reported here have been performed for a cubic sample of 216 ions (108 cations and 108 anions) in the microcanonical ensemble using periodic boundary conditions and the minimum image convention. The rigid ion Born–Mayer–Huggins–Tosi–Fumi potential model has been used. The model has the following form:

$$\phi_{ij}(r) = Z_i Z_j \frac{e^2}{r} + A_{ij} \exp[B(\sigma_i + \sigma_j - r)] - \frac{C_{ij}}{r^6} - \frac{D_{ij}}{r^8}, \quad (23)$$

where the first term represents the Coulomb interaction, the second the Born–Huggins exponential repulsion, with parameters obtained by Tosi and Fumi,⁴ and the third and fourth terms correspond to the dipole–dipole and dipole–

TABLE II. Results for the Green–Kubo coefficients of KCl. The correlation functions were evaluated from 5 ns production runs (5×10^6 time origins) and a time window of 5 ps.

T (K)	$\langle T \rangle$ (K)	ρ (g cm $^{-3}$)	L_{EE} (W/m K $\pm\epsilon$)	$L_{ZE}^2 T/L_{ZZ}$ (W/m K)
1050	1053	1.5236	0.460 ± 0.006	0.015
1100	1133	1.4945	0.444 ± 0.003	0.0063
1200	1219	1.4362	0.442 ± 0.004	0.010
1250	1231	1.4070	0.426 ± 0.007	0.0088
1300	1357	1.3779	0.390 ± 0.005	0.011

TABLE III. Comparison of the simulated electrical conductivity (σ) and thermal conductivity (λ) of NaCl with experimental data.

$\langle T \rangle$ (K)	ρ (g cm $^{-3}$)	σ^{MD} (Ω cm) $^{-1}$	σ^{expt} (Ω cm) $^{-1}$	λ^{MD} (W/m K)	λ^{expt} (W/m K)
1091	1.5420	3.50	3.63	0.609	0.516
1217	1.4878	3.95	3.93	0.58	0.493
1339	1.4335	4.21	4.17	0.55	0.471
1413	1.3793	4.25	4.31	0.505	0.458
1495	1.3250	4.23	4.44	0.493	0.443

quadrupole dispersion energies, with parameters obtained by Mayer.²³ The Ewald-sum method was used to calculate the Coulombic potential energy and forces,^{11,24} with the value $\alpha = 5.6/L$ for the convergence parameter (L is the length of the side of the MD box). The real-space part of the Ewald–Coulomb potential and the short-range interactions were truncated for $r_c = L/2$ and the Fourier part of the force and potential energy was summed up to the vector $|\mathbf{h}|_{\text{max}}^2 = 27$, with the k -space vector given by $\mathbf{k} = 2\pi\mathbf{h}/L$. The positions at time zero were defined as those corresponding to the face-centered cubic lattice of solid NaCl with the cations occupying octahedral holes, and the zero time velocities were randomly assigned and scaled to ensure a zero total linear momentum. The Verlet “leap-frog” algorithm has been used to solve Newton’s equations of motion²⁴ with a time step of 1 fs. The system was equilibrated around the desired temperature through scaling of the velocities, during the equilibration part of the simulation, 150 ps. The production stage was run for 5 ns for every point and the values of the charge and energy flux accumulated every time step. The correlation functions were built and integrated to give the values of the three transport coefficients given by Eq. (11).

IV. RESULTS

Figures 1–3 show the coefficients L_{EE} , L_{ZZ} , and L_{EZ} obtained from the integration of the energy and charge auto-correlation functions and energy and charge cross correlation function for the different state points simulated for the case of sodium chloride. The variation of the coefficients with time is given only for the first 1.5 ps but the average values have been computed up to 5 ps. The cross correlation function between the energy and charge currents was found to be the most difficult to accurately calculate because in spite of its fast convergence to zero, large fluctuations persist for some state points for the entire five million time origins used in the computation of the coefficients.

TABLE IV. Comparison of the simulated electrical conductivity (σ) and thermal conductivity (λ) of KCl with experimental data.

$\langle T \rangle$ (K)	ρ (g cm $^{-3}$)	σ^{MD} (Ω cm) $^{-1}$	σ^{expt} (Ω cm) $^{-1}$	λ^{MD} (W/m K)	λ^{expt} (W/m K)
1053	1.5236	2.40	2.19	0.445	0.387
1133	1.4945	2.61	2.38	0.438	0.374
1219	1.4362	2.80	2.56	0.432	0.359
1231	1.4070	2.80	2.59	0.417	0.357
1357	1.3779	3.03	2.84	0.379	0.336

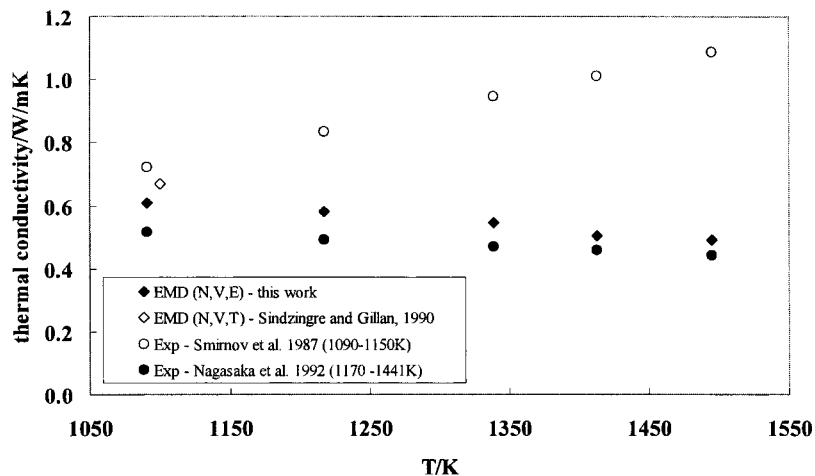


FIG. 4. Comparison of the simulated thermal conductivity at different state points with experimental and simulation data for sodium chloride.

Tables I and II give the values of the two terms of Eq. (10) involved in the calculation of the thermal conductivity of sodium and potassium chloride. It can be seen that the term in Eq. (10) involving the electrical conductivity and the cross term are much higher for NaCl for which the masses of the two ions are relatively different, than for KCl for which the masses of K^+ and Cl^- are very similar. This results from the fact that for KCl the cross term involving the charge and energy currents is much lower than for NaCl. Notice that the electrical conductivity, which is in the denominator, is lower for KCl than for NaCl and that is correctly predicted from the simulation results. Tables III and IV compare the values of the electrical conductivity and thermal conductivity with experimental data. The experimental results for the electrical conductivity are from Janz²⁵ and the thermal conductivity values are from Nagasaka *et al.*³ The electrical conductivity for NaCl is in very good agreement with the experimental data. For KCl the results are still satisfactory. The thermal conductivity is shown to agree relatively well with the experimental data in general within 10%–20%. The predicted temperature dependence is weakly negative in agreement with the results of Nagasaka *et al.*³ Figures 4 and 5 give a general comparison of the simulation results of this work with different sets of experimental data and with the simulation results of Sindzingre and Gillan.⁵ It can be seen that the

difference between the different sets of experimental data is rather large and an opposite temperature dependence is predicted.

The simulation results obtained in this work clearly show that the BMHTF potential overpredicts the thermal conductivity of NaCl and KCl and a well-defined negative temperature dependence is predicted.

V. CONCLUSIONS

Equilibrium MD simulations in the microcanonical ensemble have been performed to investigate the temperature dependence of the thermal conductivity of molten NaCl and KCl. A weak negative temperature dependence was found for the thermal conductivity of molten NaCl and KCl in agreement with the experimental results of Nagasaka *et al.*³ The results obtained are in satisfactory agreement with the available experimental data, generally overpredicted within 10%–20%.

A discussion on the form of the reciprocal space part of the potential part of the energy flux for ionic systems for which the Ewald sum is used to handle the long-range forces has been given. The expression used is relatively efficient thus permitting one to run relatively long simulations—a

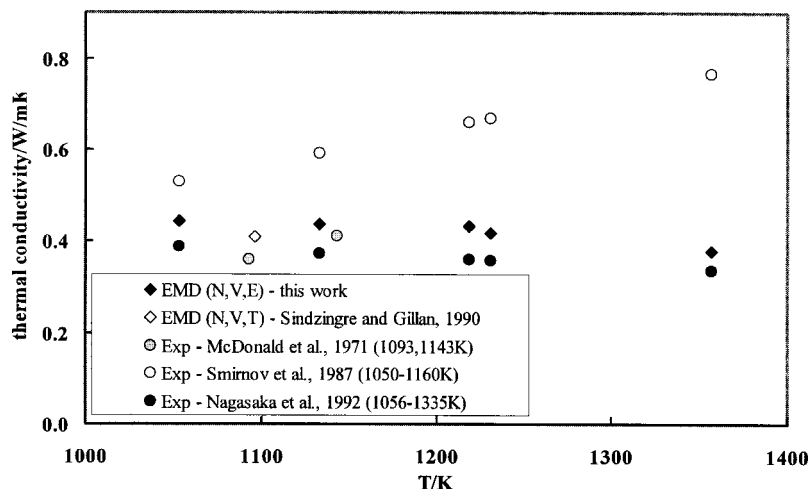


FIG. 5. Comparison of the simulated thermal conductivity at different state points with experimental and simulation data for potassium chloride.

condition normally required in the use of the Green–Kubo method to obtain a good statistical precision of the calculated correlation functions.

In analogy with the case of the shear viscosity it is expected that the inclusion of a polarization model improves to some degree the accuracy of the results. The use of polarization shell models have however the problem of greatly increasing the time of computation. This fact highly limits the applicability of shell models for the calculation of thermal conductivity for which long simulations are needed.

ACKNOWLEDGMENTS

N.G. would like to acknowledge fellowship support from Fundacao para a Ciencia e Tecnologia from Portugal for a Ph.D. grant under the program PRAXIS XXI/BD/19792/99, and to Colorado School of Mines, where part of this work was developed, for the opportunity provided as a visiting student. J.F.E. acknowledges support from the U.S. Department of Energy, Office of Science, Grant No. DE-FG03-95ER14568.

¹M. V. Smirnov, V. A. Khokhlov, and E. S. Filatov, *Electrochim. Acta* **32**, 1019 (1987).

²J. McDonald and H. T. Davis, *Phys. Chem. Liq.* **2**, 119 (1971).

³Y. Nagasaka, N. Nakazawa, and A. Nagashima, *Int. J. Thermophys.* **13**, 555 (1992).

⁴M. P. Tosi and F. G. Fumi, *J. Phys. Chem. Solids* **25**, 45 (1964); F. G. Fumi and M. P. Tosi, *ibid.* **25**, 31 (1964).

⁵P. Sindzingre and M. J. Gillan, *J. Phys.: Condens. Matter* **2**, 7033 (1990).

⁶T. Fuchiwaki and Y. Nagasaka, Proceedings of the Third KSME-JSME, Thermal Engineering Conference III-255 (1996).

⁷K. Takase and N. Othori, *Electrochem.* **67**, 581 (1999); K. Takase, I. Akiyama, and N. Ohtori, *Proc. Electrochem. Soc.* **99**, 376 (2000).

⁸B. Bernu and J. P. Hansen, *Phys. Rev. Lett.* **48**, 1375 (1982).

⁹S. Nose and M. L. Klein, *Mol. Phys.* **50**, 1055 (1983).

¹⁰D. M. Heyes, *Phys. Rev. B* **49**, 755 (1994).

¹¹M. J. L. Sangster and M. Dixon, *Adv. Phys.* **25**, 247 (1976).

¹²C. Pierleoni, G. Ciccotti, and B. Bernu, *Europhys. Lett.* **4**, 1115 (1987);

C. Pierleoni and G. Ciccotti, *J. Phys.: Condens. Matter* **2**, 1315 (1990).

¹³F. Bresme, B. Hafskjold, and I. Wold, *J. Phys. Chem.* **100**, 1879 (1996).

¹⁴S. Motoyama, Y. Ichikawa, Y. Hiwatari, and A. Oe, *Phys. Rev. B* **60**, 292 (1999).

¹⁵S. P. de Groot and P. Mazur, *Non-equilibrium Thermodynamics* (New York, 1984).

¹⁶L. Onsager, *Phys. Rev.* **37**, 405 (1931).

¹⁷R. Zwanzig, *Annu. Rev. Phys. Chem.* **16**, 67 (1965); D. A. McQuarrie, *Statistical Mechanics* (Harper & Row, New York, 1976).

¹⁸C. Hoheisel, *Theoretical Treatment of Liquids and Liquid Mixture* (Elsevier, Amsterdam, 1993).

¹⁹B. Bernu and P. Vieillefosse, *Phys. Rev. A* **18**, 2345 (1978).

²⁰B. R. A. Nijboer and F. W. De Wette, *Physica (Utrecht)* **23**, 309 (1957).

²¹D. R. Wheeler, N. G. Fuller, and R. L. Rowley, *Mol. Phys.* **92**, 55 (1997).

²²N. Galamba, C. A. Nieto de Castro, and J. F. Ely, *J. Phys. Chem. B* **108**, 3658 (2004).

²³J. E. Mayer, *J. Chem. Phys.* **1**, 270 (1933).

²⁴M. P. Allen and D. J. Tildesley, *Computer Simulations of Liquids* (Clarendon, Oxford, 1997).

²⁵G. J. Janz, Database NIST Properties of Molten Salts Database (NIST SRD 27, Boulder, 1992).